SCOTT A. GEARHART

IMAGE DEGRADATIONS OF AN AERODYNAMICALLY SHAPED OPTICAL WINDOW

Optical sensors mounted on airborne platforms require transparent windows as protection against particulates, water droplets, thermal shock, and aerodynamic loads. In most cases, however, aerodynamic window shapes act as distorting lenses that can severely degrade the sensor image. The inclined cylindrical window is an aerodynamically shaped window used in mounting sensors on the sides of vehicles. Its optical degradations are examined. In addition, the effects of a cylindrical window shape on sensor performance, as well as several optical correction techniques, are described.

INTRODUCTION

Optical sensors mounted on low-velocity platforms such as ships and propeller-driven aircraft typically include a hemispherical or flat window to protect the sensor components from the environment. Because the hemispherical window can allow much larger viewing fields, it is widely used in surveillance, mapping, and tracking applications. The optical aberrations produced by the hemispherical window are easily correctable in the sensor optical train.

For high-velocity platforms such as jet aircraft, spacecraft (during ascent or descent), and missiles, a hemispherical window produces excessive drag that limits speed and range. To overcome this problem, researchers are investigating window configurations with lower drag. In general, low-drag windows can be classified into two categories: (1) faceted windows constructed from several flat window panes, and (2) conformal windows having a single curved surface. Figure 1 shows examples of both window types.

The image degradations produced by faceted windows are minimal as long as the observed objects are far away. Faceted windows, however, require metal-to-glass (or ceramic) joints that are particularly susceptible to

thermal and aerodynamic stresses. Further, the joints cause partial obscuration of the sensor. The conformal window has structural advantages and minimizes sensor obscuration losses. Specifically, a convex surface can withstand larger loads than a flat surface, thus requiring less support. The problem with the conformal window is the severity of geometric aberrations. Optical correction is difficult because the nature and magnitude of the image distortion change with viewing angle through the window.

The inclined cylindrical window is an attractive conformal window design because it is geometrically simple and thus easy to analyze and fabricate. This article presents a brief tutorial describing the effects of window optical distortion on imaging-system performance, followed by an analysis of several cylindrical window designs and a discussion of approaches to optical correction of the window effects.

SENSOR PERFORMANCE

Light rays emanating from a distant point object are essentially parallel when they enter the sensor aperture and are focused by the sensor optics to a point in the detection plane. An inclined cylindrical window in front of
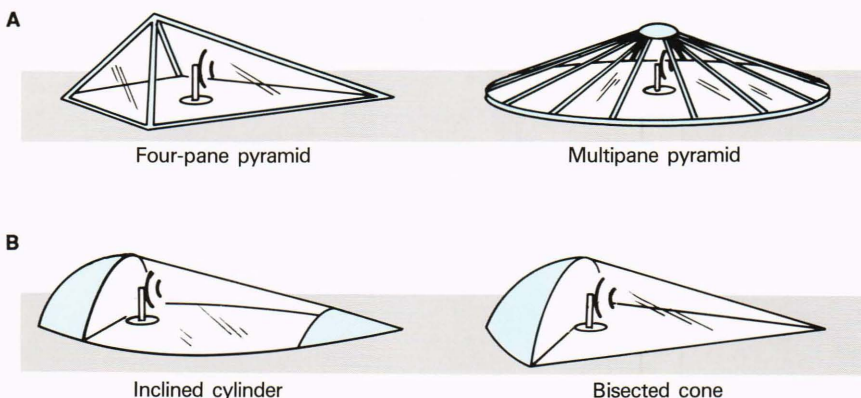
Four-pane pyramid   Multipane pyramid

Inclined cylinder   Bisected cone

Figure 1. Low-drag window configurations. A. Faceted windows. B. Conformal windows.

the sensor non-uniformly refracts the incoming rays from their parallel trajectory, with two detrimental results: reduced optical resolution and boresight error.

Optical resolution is traditionally defined as the minimum angular separation of two distant point objects necessary to recognize separate images. The criterion that defines this angular separation varies with application. One commonly used definition states that the two points are resolved when their angular separation equals the angle subtending one of the images. With this definition, the optical resolution follows directly from the point image size.

To achieve infinitely high resolution, a perfect point image would have to be formed. To form such an image, an ideal (i.e., aberration-free) imaging system would have to collect all the light rays emanating from the point object. That situation is not possible, because the limited extent of lens apertures leads to some information loss and thereby causes an image degradation. This fundamental limit on image quality is called the diffraction limit. Although the optics in many imaging sensors are of sufficient quality to provide diffraction-limited optical resolution, aberrations produced by a cylindrical window make it difficult to achieve this ideal limit. Reduced resolution decreases the sensor's ability to discern clusters of distant objects and to distinguish objects from the natural background (sun reflections, clouds, and so on).

Boresight error occurs when the line of sight from the object is perceived at an erroneous angle, causing an apparent object positional error. Changes in boresight error with viewing angle through the window as the sensor tracks can also be misconstrued as object motion. Such errors degrade the performance of mapping, pointing, or tracking systems.

Boresight error can be quantified as the sum of primary and residual components. The primary component is the angular difference between the apparent and actual lines of sight as defined by the light ray through the center of the sensor aperture (the chief ray). The residual component is typically small and results when the image is nonsymmetrically blurred such that its centroid no longer coincides with the intersection of the chief ray in the image plane. The residual boresight error is quantified as the angular difference between the image centroid and the chief-ray intersection position. Both components of boresight error are depicted in Figure 2.

Geometrically induced boresight error is a smaller problem than poor optical resolution, since it can sometimes be measured and corrected in the sensor processing electronics. For this reason, cylindrical-window correction techniques emphasize good optical resolution. Boresight errors most detrimental to sensor performance are those that change with time and cannot be easily predicted, such as errors from flow-field refraction, pressure loading, and heating.

RAY-TRACE ANALYSIS

The optical aberrations produced by the cylindrical window were analyzed with a general-purpose optical design program. Because tilted and decentered surfaces were required to model the geometry, the analysis of the

cylindrical window was unique in comparison with more standard optical design problems (e.g., the design of a zoom lens). The lack of three-dimensional graphics in the optical design program made verification of the geometric inputs difficult. Moreover, in some cases, iterative ray-trace computations failed to converge to a solution. To avoid these errors, many trial-and-error permutations of the geometric inputs and ray trajectories were required.

Five windows of various thicknesses and diameters were analyzed. An $f/5$, two-mirror, Cassegrain-type reflecting telescope with a 5.1-cm aperture was used to model the sensor imaging optics, as shown in Figure 3. The telescope was pivoted on a point located on the window longitudinal axis to maintain rotational symmetry.
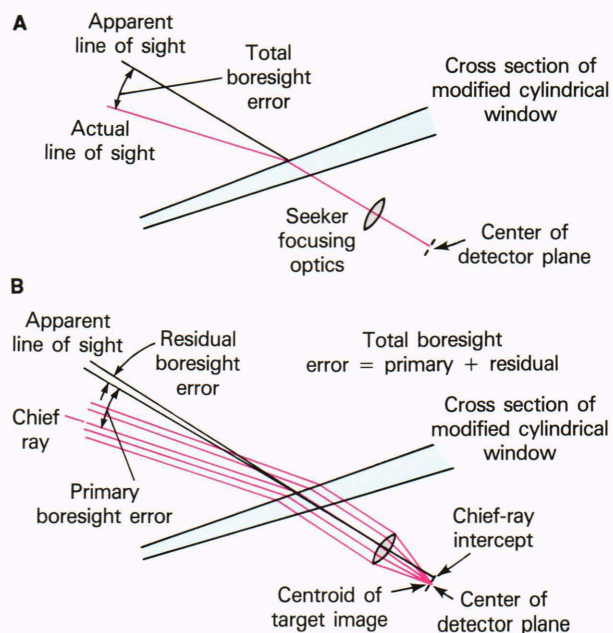

Figure 2. Boresight error caused by window refraction. **A**. Total boresight error. **B**. Primary and residual components of the total boresight error.
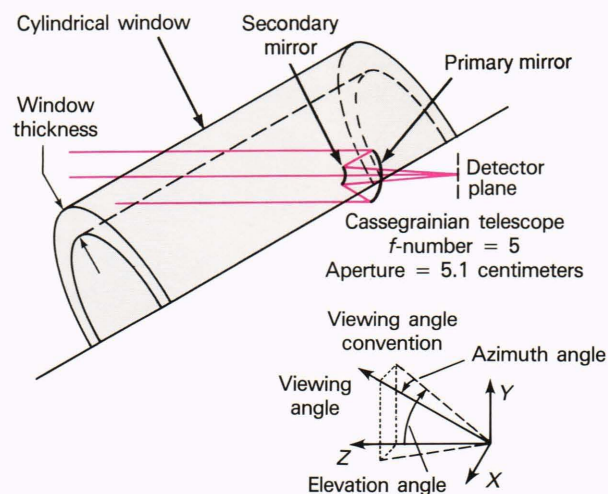

Figure 3. Geometry of ray-trace analysis. The azimuth angle is designated in the elevation plane.

A window refractive index of 1.7 was used. The telescope design provided diffraction-limited optical resolution at infrared wavelengths over a 2° field of view.

The analysis was performed by analytically tracing parallel rays from an infinitely distant ideal point source through the window/telescope combination at various viewing angles. The intersections of the rays from a distant point object were plotted in the telescope image plane to define the shape and size of the point image. The result of this process was a pictorial representation of the image called a spot diagram. The diameter of the circle containing 90% of the light-ray intersection points was used to define the image size (i.e., spot size). Consistent with the definition given previously, the angular optical resolution is given by

$$a \approx d/f ,$$

where *d* is the spot size and *f* is the effective focal length of the telescope.

Figures 4A and 4B show two spot diagrams obtained at the two viewing angles indicated. The elongation of the images in one direction is characteristic of window astigmatism. Astigmatism occurs when the magnifying powers along two axes of an optical system differ. The elongation occurs because the light rays through the horizontal axis of the telescope (the sagittal rays) are focused at a longer distance than the rays through the vertical axis (the meridional rays). The differences in size and orientation of the elongation demonstrate that the window astigmatism is strongly dependent on the viewing angle.

Placing the telescope pivot point on the longitudinal axis of the window greatly simplifies the form of the window aberrations. Because of rotational symmetry, no primary boresight errors occur, and window aberrations can be attributed primarily to astigmatism dependent on elevation angle. If the telescope pivot is moved off the window axis closer to the window, an additional aberration appears at nonzero azimuth viewing angles. This feature is apparent when the larger astigmatic component is removed at a particular viewing angle with a simple cylindrical lens. Figure 5 shows the result of a spot diagram for this configuration at an elevation angle of 25° and an azimuth angle of 46°. The shape of the image is similar to that characteristic of coma commonly observed in axially symmetric optical systems. Moving the telescope pivot off the window axis also results in boresight errors.

Because of the variable (angle-dependent) astigmatism, a simple cylindrical lens placed in the front of the telescope cannot provide good resolution for all viewing angles. This situation is apparent from the ray-trace results presented in Table 1 for a 12.7-cm-diameter, 0.25-cm-thick window. The second column in Table 1 gives the optical resolution without any form of optical correction, and the third column gives the resolution that results from using a simple cylindrical correction lens (with the telescope pivot point on the window axis). Good resolution with this particular lens occurs at a viewing angle of 17°. At angles below 17°, however, the
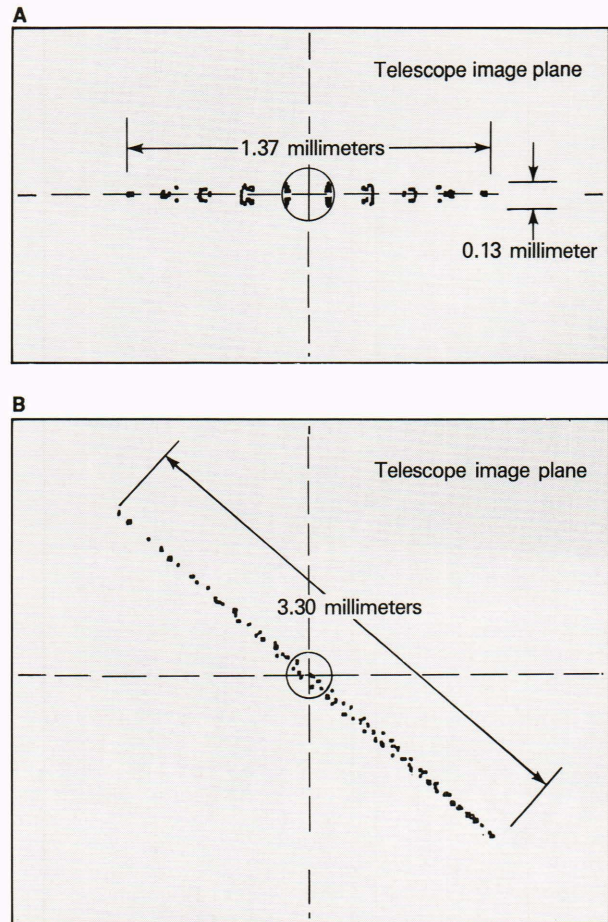
Figure 4. Elongation of point images caused by window astigmatism. The individual dots are the image locations of optical rays uniformly spaced at the entrance pupil. The magnitude and orientation of the image degradation vary with viewing angle. **A.** Elevation angle = 0°, azimuth angle = 0°. **B.** Elevation angle = 25°, azimuth angle = 46°.
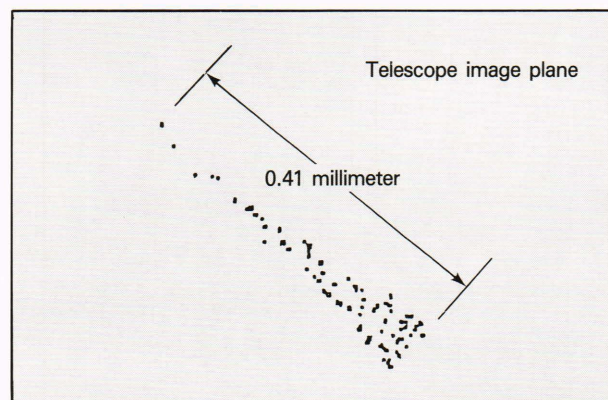
Figure 5. Coma-like aberration that remains after astigmatic correction when the telescope is 3.81 cm above the window axis. This aberration occurs only for nonzero azimuth viewing angles. The window is 19 cm in diameter and 0.25 cm thick. Elevation angle = 25°, azimuth angle = 46°.

Table 1. Optical correction using a single cylindrical lens.

Elevation angle (degrees)	Optical resolution (mrad)[a]	
	Without correction	With correction
0	3.83	4.24
17	6.17	0.48
34	7.13	1.43
51	7.45	1.93

Note: Data are for a 12.7-cm-diameter, 0.25-cm-thick window.
[a]The diffraction-limited resolution at 5 μm is about 0.25 mrad.

Table 2. Optical correction using an adaptive power lens.

Elevation angle (degrees)	Optical resolution (mrad)[a]	
	Without correction	With correction
0	2.59	0.39
17	4.15	0.37
34	4.79	0.35
51	4.99	0.36

Note: Data are for a 19.0-cm-diameter, 0.25-cm-thick window.
[a]The diffraction-limited resolution at 5 μm is about 0.25 mrad.

lens does not provide enough power; at angles above 17°, the lens provides too much power.

OPTICAL CORRECTION

The preceding analysis indicates that acceptable optical resolution can be achieved by locating the telescope pivot point near the window longitudinal axis and removing the astigmatism that is dependent on the viewing angle. Two approaches for removing window astigmatism can be used. One technique is to actively correct the astigmatism as the viewing angle changes. Figure 6 depicts one correction assembly composed of two cylindrical lenses, one having positive power and the other having negative power. The power and orientation of astigmatic correction are varied by rotating the lenses relative to each other. A slight shift of the image plane is required to optimize the telescope focus as a function of viewing angle. Table 2 shows that good optical resolution can be achieved at the center of the telescope field of view for a 19.0-cm-diameter, 0.25-cm-thick window at the specified elevation angles. Because of rotational symmetry, azimuth angles do not need to be consid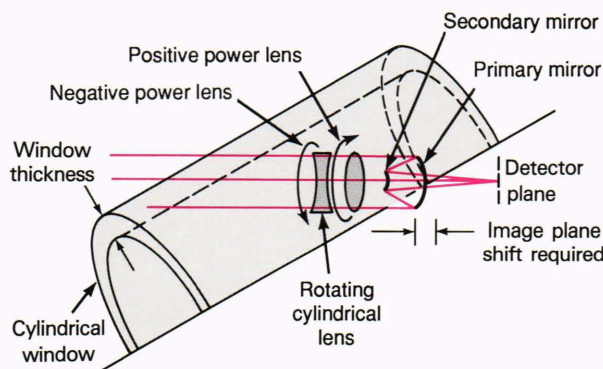ered. A similar technique might incorporate three or more cylindrical elements. The power could be varied by changing the element spacing similar to that of a zoom lens. The orientation of correction would be changed by rotating the entire assembly.

The mechanical implementation of an active correction technique may be difficult in applications where the sensor must rapidly scan a search area and where size, weight, and power restrictions apply. An approach that significantly reduces the required mechanical complexity is to modify the window surfaces to achieve a constant astigmatism with viewing angle. The resulting constant residual astigmatism can be removed with a simple cylindrical lens in front of the imaging optics; the lens rotates to the correct orientation as the telescope azimuth angle changes.

Figure 7 illustrates an appropriate window modification combined with a cylindrical lens in front of the telescope. The inner window surface is a section of a cone whose taper angle with respect to the outer cylindrical surface is determined to produce a nearly constant amount of astigmatism for all viewing angles. Table 3 shows ray-trace results before and after correction for five window configurations. For all but one window, optical resolution of 1 mrad or less at the center of the tele-
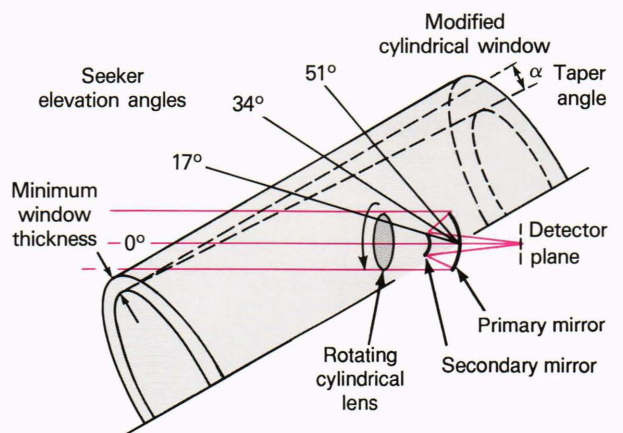

Figure 6. Astigmatic correction assembly composed of two cylindrical lenses. The lenses rotate relative to each other as viewing angle changes to vary the power and orientation of astigmatic correction.

Figure 7. Astigmatic correction assembly composed of a modified cylindrical window and a cylindrical lens. The modified window surface makes astigmatism constant with viewing angle. The lens rotates as viewing angle changes to remove constant residual astigmatism.

Table 3. Optical correction using a modified cylindrical window.

Window size (cm)			Optical resolution (mrad)[a]	
Diameter	Thickness	Elevation angle (degrees)	Without correction	With correction
19.0	0.25	0	2.59	0.36
		17	4.15	0.39
		34	4.79	0.31
		51	4.99	0.31
19.0	0.51	0	5.31	0.55
		17	8.54	0.43
		34	9.85	0.92
		51	10.26	0.92
15.2	0.25	0	4.14	0.92
		17	6.69	0.91
		34	7.72	0.47
		51	8.06	0.39
15.2	0.51	0	8.59	1.90
		17	13.85	1.09
		34	16.03	1.56
		51	16.74	1.81
12.7	0.25	0	3.83	1.06
		17	6.17	0.96
		34	7.13	0.81
		51	7.45	1.05

[a]The diffraction-limited resolution at 5 μm is about 0.25 mrad.

Table 4. Optical resolution at the center and edge of the telescope field of view after correction.

	Optical resolution (mrad)[a]	
Elevation angle (degrees)	Center of field of view	Edge of field of view
0	1.06	1.98
17	0.96	1.33
34	0.81	—
51	1.05	—

Note: Data are for a 12.7-cm-diameter, 0.25-cm-thick window.
[a]The diffraction-limited resolution at 5 μm is about 0.25 mrad.

scope field of view is achievable over all viewing angles. The degree of correction achieved decreases as the window diameter decreases and thickness increases.

Thus far, optical resolution at the center of the telescope field of view has been considered. Ray-trace results from an earlier study indicate that spot sizes less than 1 mrad can be achieved for the 19.0-cm-diameter, 0.25-cm-thick window at the edge of the 2° field of view. Table 4 shows that despite attempts at optical correction of the 12.7-cm-diameter, 0.25-cm-thick window, the resolution at the edge of the telescope field of view is substantially poorer than at the center. The data were obtained at the worst-case viewing angles. If a given application requires a window of this size, better performance at the edge of the telescope field of view can be achieved by increasing the window inclination angle (15° was used in this study), decreasing the window thickness, and reducing the telescope aperture.

Modifying the inner window surface causes geometrically induced boresight errors that must be electronically compensated in the sensor processor. For the 12.7-cm-diameter, 0.25-cm-thick window, boresight errors as high as 1.0° are induced at 0° elevation. This error reduces to about 0.2° as the elevation increases to 51°.

SUMMARY

The feasibility of an optical sensor/cylindrical window combination can be assessed only by carefully considering the system requirements. For example, the platform aerodynamic requirements will affect the slope and diameter specifications of the cylindrical window. The projected stress and thermal environment will determine the required window thickness. Finally, the system detection requirements will influence the sensor aperture size, instantaneous field of view, and optical resolution. A trade-off evaluation of each of these factors for several applications is currently under way.

The issue of window fabrication has not been addressed. Because of recent advances in diamond-machining technology, investigators expect that prototype windows for infrared wavelengths can be fabricated, although the manufacturing specifications that dictate optical quality have not been identified. This issue, as well as other producibility concerns, will be the subject of later studies.

THE AUTHOR
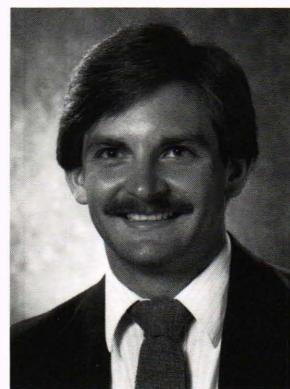
SCOTT A. GEARHART graduated from the Pennsylvania State University in 1982 with a B.S. degree in engineering science. He received an M.S. degree in electrical engineering from The University of Maryland in 1987. Mr. Gearhart joined APL in 1983 and has worked primarily on the development and evaluation of optical and infrared sensors for guidance and surveillance applications. He has also participated in IR&D efforts in optical radar processing and laser remote sensing, as well as biomedical studies in laser angiography and laser Doppler velocimetry of simulated blood flow.